CHEMMEDCHEM

DOI: 10.1002/cmdc.200500039

Highly Potent and Specific GSK-3β Inhibitors That Block Tau Phosphorylation and Decrease α-Synuclein Protein Expression in a Cellular Model of Parkinson's Disease

Alan P. Kozikowski,*[a] Irina N. Gaisina,[a] Pavel A. Petukhov,[a] Jayalakshmi Sridhar,[a] LaShaunda T. King,[b] Sylvie Y. Blond,[b] Tetyana Duka,[c] Milan Rusnak,[c] and Anita Sidhu[c]

*Research by Klein and co-workers suggests that the inhibition of GSK-3β by small molecules may offer an important strategy in the treatment of a number of central nervous system (CNS) disorders including Alzheimer's disease, Parkinson's disease, and bipolar disorders. Based on results from kinase-screening assays that identified a staurosporine analogue as a modest inhibitor of GSK-3β, a series of 3-indolyl-4-indazolylmaleimides was prepared for study in both enzymatic and cell-based assays. Most strikingly, whereas we identified ligands having poor to high potency for GSK-3β inhibition, only ligands with a K_i value of less than 8 nM, namely maleimides **18** and **22**, were found to inhibit Tau phosphorylation at a GSK-3β-specific site (Ser 396/404). Accordingly, maleimides **18** and **22** may protect neuronal cells against cell death by decreasing the level of α-Syn protein expression. We conclude that the GSK-3β inhibitors described herein offer promise in defending cells against MPP^+-induced neurotoxicity and that such compounds will be valuable to explore in animal models of Parkinson's disease as well as in other Tau-related neurodegenerative disease states.*

Introduction

It is now well-appreciated that many disease pathways involve abnormal regulation of phosphorylation events, and to date, a variety of kinase inhibitors have proven effective in the treatment of certain forms of cancer. As there are estimated to be approximately 600 protein kinases and ≈80 phosphatases,[1] a large number of potential targets are present toward which drug discovery efforts can be directed. Whereas early efforts in the kinase inhibitor field focused on the design of molecules selective for a single kinase, recent findings suggest that the development of compounds which target more than a single kinase may lead to the discovery of more efficacious drugs. This design strategy is based in part on preventing cells from developing resistance to the kinase inhibitor through mutations that give rise to changes in the amino acid residues present in the active site.

In the work described herein, we directed our attention to the discovery of inhibitors of the glycogen synthase kinase-3β (GSK-3β), as the research results of Klein and others suggest the possibility to use such inhibitors in the treatment of a number of CNS disorders including Alzheimer's disease (AD),[2] Parkinson's disease, bipolar disorders,[3,4] and even traumatic brain injury. In humans, two genes are present that encode the related GSK-3 isoforms GSK-3α and GSK-3β, which exhibit approximately 98% sequence identity within their catalytic domains. It now appears that GSK-3-induced increases in the level of β-catenin and nuclear translocation play a role in the signal-transduction cascade in which β-catenin may regulate the expression of genes involved in adult neurogenesis, neuroplasticity, and ultimately, behavioral alterations beneficial in the treatment of mood disorders.

Our work in this area was influenced by the maleimide-bearing natural product staurosporine, which is a compound that was first identified as having inhibitory activity toward protein kinase C (PKC), although it is now known to be rather promiscuous in its activity; it is able to block other protein kinases. Over the years, a variety of staurosporine analogues have been synthesized and optimized for the inhibition of several different kinase targets, including GSK-3β.[5–9] However, the SAR pat-

[a] *Prof. Dr. A. P. Kozikowski, Dr. I. N. Gaisina, Prof. Dr. P. A. Petukhov, Dr. J. Sridhar*
Drug Discovery Program, College of Pharmacy
University of Illinois at Chicago
833 S. Wood St., Chicago, Illinois 60612 (USA)
Fax: (+1) 312-996-7577
E-mail: kozikowa@uic.edu

[b] *Dr. L. T. King, Prof. Dr. S. Y. Blond*
Center of Pharmaceutical Biotechnology
University of Illinois at Chicago
900 S. Ashland Ave., Chicago, Illinois 60612 (USA)

[c] *Dr. T. Duka, Dr. M. Rusnak, Prof. Dr. A. Sidhu*
Laboratory of Molecular Neurochemistry
Georgetown University Medical Center
3970 Reservoir Rd., Washington, DC 20007 (USA)

terns we have observed for some of these maleimides are unique, with the biological activity found in the Parkinson's disease cell models significant and highly dependent on the observed K_i values for GSK-3β inhibition.

Results and Discussion

Identification of 3-indolyl-4-indazolylmaleimides as potent GSK-3β inhibitors: synthesis and screening

Initially, in an effort to develop some analogues of staurosporine as inhibitors of 3-phosphoinositide-dependent protein kinase-1 (PDK-1),[10] we screened a number of staurosporine-based structures composed of two indole rings, one indazole ring, and one indole ring or two indazole rings against a family of 30 kinases. Of the compounds tested, we found that one, the indolyl-indazolylmaleimide (Figure 1), was able to inhibit 98% of the kinase activity of GSK-3β at a concentration of 10 μM.

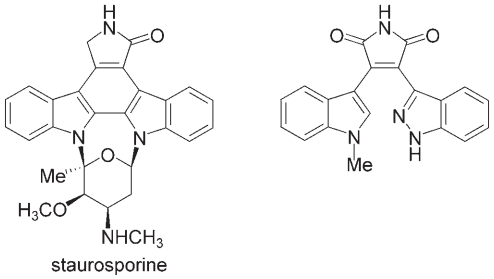

Figure 1. Lead candidate inhibitor (right) of GSK-3β discovered through a kinase screening study.

At that time, the connection had already been made between the mood-stabilizing action of lithium and its ability to inhibit GSK-3β (with a K_i value of 2 mM) by Klein and co-workers,[3,11] and we elected to further explore the SARs of this compound to discover more potent versions of our lead candidate. Accordingly, a series of 3-indolyl-4-indazolylmaleimides was prepared by using the methods given in Scheme 1. The selection of new compounds for synthesis was guided in part by structure-based modeling methods in conjunction with general principles of medicinal chemistry.

The 3-(indol-3-yl)-4-(1*H*-indazol-3-yl)maleimide-based ligands **5**–**35** were prepared by condensation of the indolyl-3-glyoxylate esters **3** and the indazolyl-3-acetamides **4**[12] (Scheme 1). *N*-Alkylation of indoles **1** with various alkyl halides in the presence of sodium hydride followed by acylation of the resulting indoles **2** with oxalyl chloride and then ester formation afforded the precursors **3**. The required reaction partners, the indazolyl-3-acetamides **4**, were prepared from the appropriate *ortho*-nitrobenzaldehyde according to a previously published procedure.[13,14] The appendage of an alkyl side chain onto the indazole ring (as in compound **11**) was carried out by treatment of the acetamides **4** with 2-bromoethyl methyl ether in

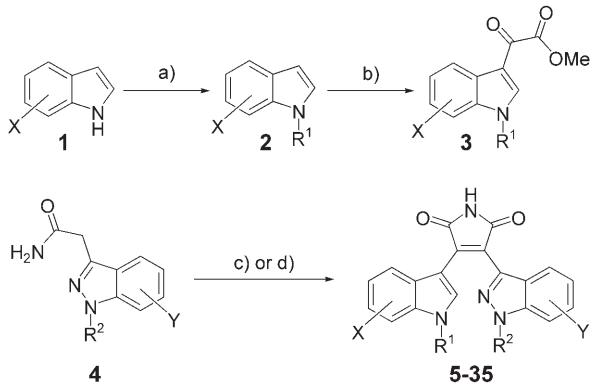

Scheme 1. Synthesis of 3-indolyl-4-indazolylmaleimides: a) alkyl halide, NaH, *N*,*N*-dimethylformamide (DMF); b) $(COCl)_2$, Et_2O, then NaOMe; c) **3**, *t*BuOK, THF; d) 1. $CH_3O(CH_2)_2Br$, NaH, DMF, 2. **3**, *t*BuOK, THF.

the presence of sodium hydroxide followed by column chromatography.

The new compounds were then screened for their potency to inhibit GSK-3β. Briefly, recombinant human His_6-GSK-3β (53 nM) produced in our laboratories or commercially available human GSK-3β (21 nM) was assayed for the ability to phosphorylate the pGSM peptide substrate (RRRPASVPPSPSLSRHSSHQRR; 10 μM) in the presence of the maleimides at various concentrations (0–50 μM). For comparison, we also determined the K_i values of the known GSK-3β inhibitors SB-415286 and SB-216763. As presented in Table 1, the K_i values vary from poor (4500 nM) to excellent (2 nM).

Unique SAR exhibited by the bromo- and fluoro-substituted 3-(indol-3-yl)-4-(1*H*-indazol-3-yl)maleimides analyzed by docking experiments

Of particular interest in this series are the differences in activity between the bromo- and fluoro-substituted 3-indolyl-4-indazolylmaleimides, which either contain or lack an *N*-methyl substituent on the indole nitrogen atom. As is apparent in Figure 2, the presence of the *N*-methyl group has opposite effects on GSK-3β activity. The *N*-methyl group enhances activity for the brominated ligand, but decreases the activity of the fluorinated ligand. To understand this apparent anomaly, we made use of docking experiments and the known crystal structure of GSK-3β (Figure 2).

According to these experiments, the 5-fluoro substituent in the indole ring of compounds **18** and **19** occupies a position close to the amino group of the positively charged Lys 85, while the indazole ring engages in lipophilic contact with Tyr 134 and Ile 62. Unlike the 5-fluoro substituent, the larger 5-bromo substituent in compounds **21** and **22** cannot occupy the same position, as the larger bromo group would clash with the side chains of Leu 132 and Lys 85. Instead, ligands **21** and **22** shift their position slightly to avoid this steric clash, and the 5-bromo substituent of **21** and **22** slides inside the relatively lipophilic pocket formed by the lipophilic portions of Glu 97, Leu 130, Leu 132, Val 110, Met 101, Phe 201, Cys 199, and Lys 85. Overall, the 5-fluoro-substituted ligands **18** and **19** are

Table 1. GSK-3β inhibition by substituted maleimides, SB ligands, and LiCl.

Compd	X[b]	Y	R1[c]	R2	IC_{50} [μM]	K_i [nM]
LiCl					2000	3.33×10^6
SB-415286					1.3	180
SB-216763					0.050	35
bis-indole-maleimide					1.3	225[a]
5	H	H	H	H	12.0	2250[a]
6	H	H	CH_3	H	2.6	433
7	H	H	$(CH_2)_3OTr$	H	27	4500
8	H	H	$(CH_2)_3OH$	H	1.8	300
9	H	H	$(CH_2)_2OCH_3$	H	2.5	417
10	H	H	CH_3	CH_3	0.120	80
11	H	H	CH_3	$(CH_2)_2OCH_3$	0.049	33
12	CN	H	H	H	0.081	54
13	5-NO_2	H	CH_3	H	0.46	57[a]
14	5-NO_2	H	$(CH_2)_2OCH_3$	H	0.052	35
15	5-Cl	H	CH_3	H	1.1	183
16	5-Cl	H	$(CH_2)_3OH$	H	5.0	833
17	5-Cl	H	$(CH_2)_2OCH_3$	H	0.38	41[a]
18	5-F	H	H	H	0.0114	7.6
19	5-F	H	CH_3	H	0.049	33
20	5-F	H	$(CH_2)_2OCH_3$	H	0.036	24
21	5-Br	H	H	H	0.850	567
22	5-Br	H	CH_3	H	0.0035	2.3
23	5-F	5-Cl	$(CH_2)_2OCH_3$	H	0.165	110
24	5-OBn	H	CH_3	H	1.2	200
25	5-OBn	H	$(CH_2)_3OH$	H	0.100	67
26	5-OBn	H	$(CH_2)_2OCH_3$	H	0.130	87
27	5-OBn	5-Cl	$(CH_2)_2OCH_3$	H	0.750	500
28	6-NO_2	H	CH_3	H	1.3	200
29	6-Cl	H	CH_3	H	3.1	517
30	6-F	H	H	H	0.535	357
31	6-CH_3	5-Cl	$(CH_2)_2OCH_3$	H	2.4	1600
32	6-OBn	H	$(CH_2)_2OCH_3$	H	0.450	300
33	7-OBn	H	$(CH_2)_2OCH_3$	H	0.400	267
34	H	5-Cl	CH_3	H	3.1	517
35	H	5-Cl	$(CH_2)_3OH$	H	3.6	600

[a] K_i values are the average of experiments performed at both 10 and 100 μM ATP. The apparent equilibrium dissociation constants of the inhibitors (K_i) were estimated with the Cheng–Prusoff equation and a K_M for ATP equal to 20 μM. [b] Bn = benzyl. [c] Tr = triphenylmethyl.

more exposed to the solvent, whereas **21** and **22** are inserted more deeply into the binding pocket. This is consistent with the 4.3-fold difference in activity between ligands **18** and **19**—both compounds are equally exposed to the solvent, but the NH group of the indole ring in **18** is better solvated than the corresponding *N*-methyl group in the indole ring of **19**. The respective NH and *N*-methyl groups of the 5-brominated ligands **21** and **22** are less exposed to the solvent, and they make tighter contact with the binding site. The relatively lipophilic *N*-methyl group of **22** forms a favorable contact with the lipophilic area formed by Val70. The less lipophilic NH group of **21**, on the other hand, cannot form similar interactions, and it is also somewhat close to the positively charged amino group of Lys85. Together these differences decrease the inhibitory activity of ligand **21** by ≈250-fold relative to that of ligand **22**. This fascinating aspect of the SAR is worth probing further, as such structural differences may be used to adjust the overall kinase selectivity as well as the cellular biology (including ADMET parameters) of these inhibitors.

GSK-3 and CNS disorders: inhibition of Tau phosphorylation at Ser396/404 in a cellular model of Parkinson's disease by selected 3-(indol-3-yl)-4-(1*H*-indazol-3-yl)maleimides

In pursuing the possible clinical applications of the GSK-3β inhibitors that we identified, we next investigated their action in certain cellular models relating to neuroprotection. It is well-established that the Tau protein is the main component of paired helical filaments (PHFs), aberrant structures that develop in the brain of patients with a number of late-onset neurodegenerative disorders, including Alzheimer's disease and other tauopathies such as front temporal dementia and parkinsonism associated with chromosome 17 (FTDP-17).[15,16] Hyperphosphorylation of Tau is thought to result in the destabilization of microtubles (MTs), giving rise to a "pretangle" stage[17] and subsequent loss of dendritic MTs and synapses, cytoskeletal destabilization, and eventually cell death.[18] GSK-3β phosphorylates the majority of sites on Tau which become abnormally hyperphosphorylated in PHFs, as shown both in cell culture[19] and in rodents.[20,21] GSK-3β is located at the convergence of pathways involved in AD-like Tau hyperphosphorylation.[22–28] Induction of GSK-3β transgene expression in the brain causes adult mice to develop hyperphosphorylated Tau at the PHF-1 site (phospho-epitope at Ser396/404),[29] a site critical for PHF formation that represents a specific phosphorylation site on Tau in AD brain.[30] Transgenic mice that overexpress GSK-3β also develop pretangle structures in the hippocampus, and experience increased neuronal death, gliosis, and spatial learning deficits in the Morris water maze.[31] It has also been shown that filaments resembling PHFs assemble when Sf9 cells overexpress FTDP-17 Tau (a form of Tau which includes three major mutations (G272V, P301L, and R406W)). The amount of these polymers is decreased in lithium-treated cells, which suggests that phosphorylation of FTDP-17 Tau by GSK-3β induces a conformational change favoring the formation of fibrillar polymers.[32] Moreover, a growing body of evidence suggests that GSK-3β is an important modulator of apoptosis.[33–35] The increase in GSK-3β activity precedes the induction of apoptosis. GSK-3β sits at the convergence of several signaling pathways that are critical for neuronal viability and proper function. Several apoptotic stimuli including Aβ peptide, ischemia, and excitotoxicity appear to be involved in pathways that activate GSK-3β.[29]

Thus, GSK-3 appears to be associated with a multitude of adverse events linked to MT dynamics, neurotic dystrophy, PHF-Tau, plasticity, cognitive deficits, neurodegeneration, and potentially amyloid production. Given the significant role of GSK-3β in a variety of processes linked to pathophysiological mechanisms related to AD and other CNS disorders, GSK-3 inhibition with small-molecule inhibitors affords a testable hypothesis which may be readily translated to the clinic.

Recent studies by our research group have shown that the PD-linked neurotoxin MPTP (*N*-methyl-4-phenyl-1,2,3,6-tetrahydropyridine) induces the hyperphosphorylation of Tau in a

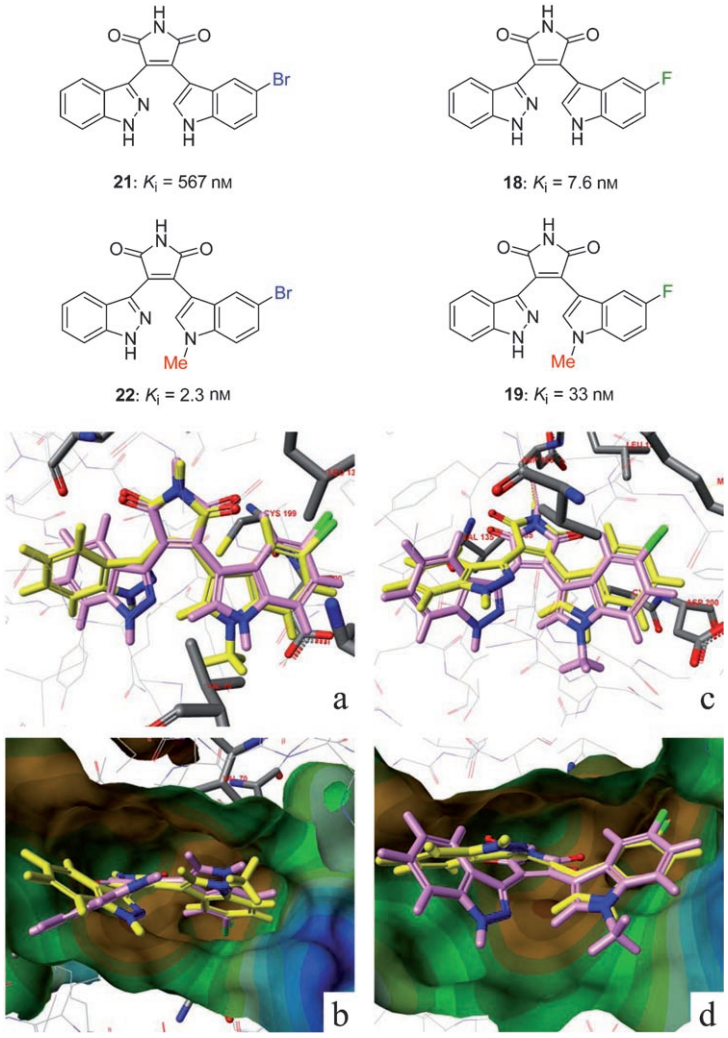

Figure 2. Compounds **18**, **19**, **21**, and **22** docked to the ATP-binding site of GSK-3β: a) **21** (rose) and **22** (yellow); b) another projection of **21** and **22**. The protein surface inside the binding site is colored by lipophilic potential (blue = hydrophilic, brown = lipophilic); c) **19** (rose) and **18** (yellow); d) another projection of **19** and **18**.

manner dependent on both the dopamine transporter and α-synuclein (α-Syn). Several of the novel GSK-3β inhibitors identified from the chemistry efforts presented herein were examined for their capacity to interfere with two of the regulated processes that play an important role in the MPP^+-induced model of neurodegeneration: Tau phosphorylation at the PHF-1 binding site (PHF-Tau; the epitope which belongs to AD-like Tau antigenicity) and α-Syn-induced toxicity. (MPP^+ is an active metabolite of MPTP.) In our studies, treatment with MPP^+ (50 μM, 48 h) induces PHF-Tau immunoreactivity. The Tau immunoreactivity was studied biochemically in two ways: through Western blot analysis by using the PHF-1 antibody, which recognizes a Tau phospho-epitope at Ser396/404 in extracts from MPP^+-treated mesencephalic neurons (Figure 3a); and through the use of SHSY5Y cells stably transfected with wild-type α-Syn (SHα-Syn cells), and transiently co-transfected with the human dopamine transporter (hDAT) cDNA (SHα-Syn/hDAT cells) (Figure 4a). Immunodetection of PHF-Tau revealed that lysates from MPP^+-treated mesencephalic primary neurons and SHα-Syn/hDAT cells were almost twice as immunoreactive for PHF-1 than those obtained from vehicle-treated cells. We next analyzed the action of six of our GSK-3β inhibitors on the formation of PHF-1 in the presence of MPP^+. Whereas no significant change in the immunoreactivity toward PHF-1 in MPP^+-treated neurons or SHα-Syn/hDAT cells was observed in the presence of compounds **8** (K_i = 300 nM), **14** (K_i = 35 nM), **16** (K_i = 833 nM), or **19** (K_i = 33 nM), a strong decrease in PHF-Tau levels was observed after treatment with either **18** (K_i = 7.6 nM) or **22** (K_i = 2.3 nM). These data appear to correlate with the in vitro potency of these ligands as GSK-3β inhibitors. Indeed, PHF-1 immunoreactivity was decreased in mesencephalic neurons by 102 and 90% relative to the corresponding MPP^+-treated groups, with compounds **18** and **22**, respectively, whereas the respective analogous decreases were 104 and 78% in SHα-Syn/hDAT cells (Figures 3a and 4a). Moreover, the potent GSK-3β inhibitors **18** and **22** led to effects similar to those observed with lithium (1 mM) on the MPP^+-induced alterations in PHF-Tau levels, both in neurons and in the transfected neuroblastoma cells (data not shown). The total Tau levels in the neurons and SHα-Syn/hDAT cells under MPP^+ exposure (by using the phosphorylation-independent antibodies Tau5) were approximately the same under all experimental conditions. The PHF-1/Tau5 ratio was measured by densitometric scanning, and the results are shown in the lower panel (Figure 3a and 4a). Data shown reflect the mean values ± SD from three independent experiments.

It has been shown that the α-Syn protein is essential to MPTP (MPP^+)-induced neurotoxicity. Moreover, specific deletion of the *α-syn* gene by homologous recombination techniques appears to attenuate the degeneration of nigrostriatal dopaminergic neurons following acute and subchronic MPTP administration.[36,37] α-Syn has been suggested to modulate dopamine (DA) homeostasis by regulating DA vesicular storage, uptake, synthesis, and release.[38–40] Results from a subchronic MPTP rodent model study[41] revealed that the loss of striatal DA concentrations and VMAT-2 protein expression following subchronic and prolonged, chronic MPTP treatment is attenuated in mice lacking α-Syn.

In the study reported herein, we demonstrated that treatment with MPP^+ also results in an increased α-Syn protein expression in mesencephalic primary neurons (Figure 3b) and in SHα-Syn/hDAT neuroblastoma cells (Figure 4b). The mean density of α-Syn relative to that of β-actin (used as a control for protein loading) increased by 68% in primary neurons and by 47% in SHα-Syn/hDAT after MPP^+ treatment, in comparison with the corresponding vehicle-treated control cells. Surprisingly, in the presence of compounds **18** and **22**, no significant increase in α-Syn level relative to that of β-actin was detected after MPP^+ exposure, in comparison with control (vehicle-

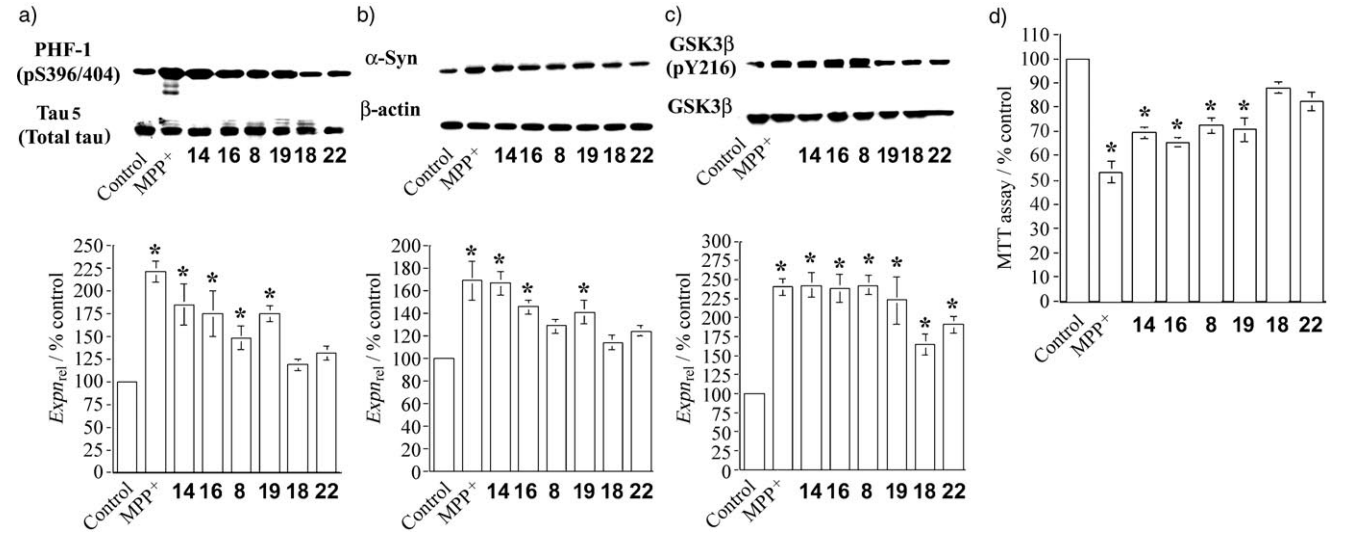

Figure 3. Cellular changes in mesencephalic neurons after treatment with MPTP and GSK-3β inhibitors. Expression levels of a) PHF-Tau, b) α-Syn, and c) *p*-GSK-3β were assessed by Western blots of the control and MPP^+-treated mesencephalic neurons in the presence or absence of specific GSK-3β inhibitors. Results in part d) show cell viability measured by the MTT cell-viability assay. Three independent experiments were performed with embryonic rat ventral mesencephalic neuronal cultures. One timed-pregnant rat at gestational day 16 was used per experiment. Mesencephalic neurons were treated with MPP^+ (50 μM) for 48 h or with vehicle in DMSO (0.2% *v/v*) in the presence or absence of the GSK-3β inhibitors (1 μM added for the last 16 h of MPP^+ exposure). The lower panel in each individual part shows quantitation of the results, obtained by measuring the optical density of each band. These are expressed as the ratio of the densities between a) PHF-Tau and total Tau, b) α-Syn and β-actin, and c) *p*-GSK-3β(Y216) and GSK-3β. Values from each treatment are expressed as the mean ± SD. The significance of difference relative to the respective vehicle-treated groups (which were set at 100%) was determined by the Student's *t*-test (*$p \leq 0.05$ for immunoblot analysis; *$p \leq 0.01$ for MTT assay).

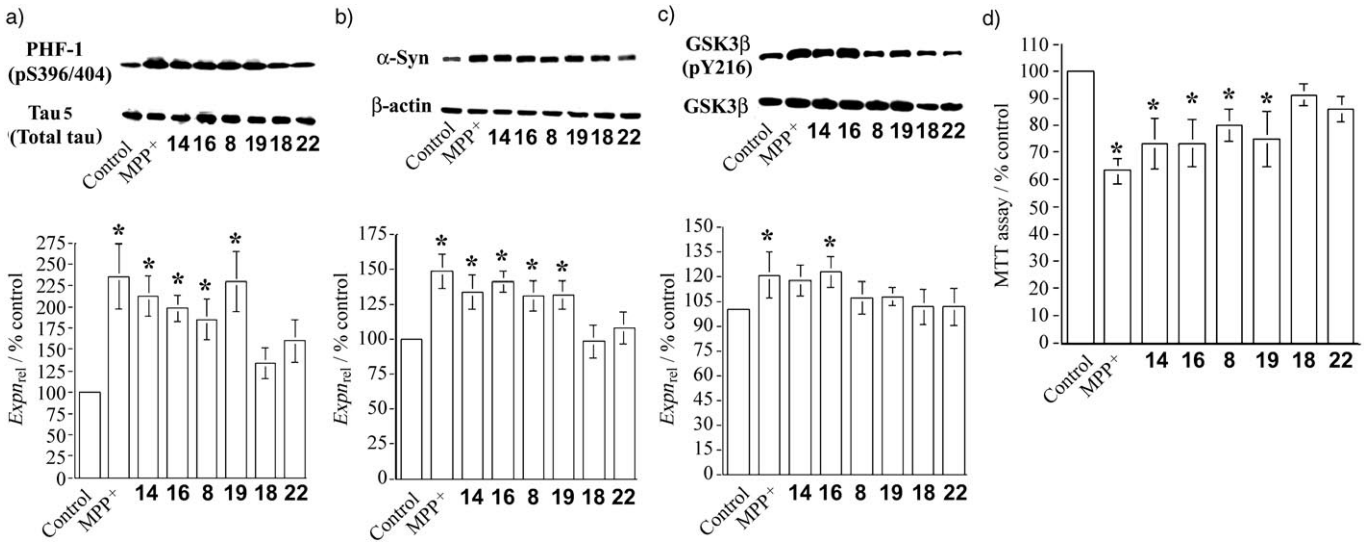

Figure 4. GSK-3β Hyperphosphorylation of Tau is dependent on the presence of both DAT and α-Syn. Immunoblot analysis of the expression levels of Tau phosphorylated at a) Ser396/404, b) α-Syn, and c) *p*-GSK-3β evaluated from cell lysates of vehicle- or MPP^+-treated SHSY5Y neuroblastoma cells stably transfected with wild-type α-Syn (SHα-Syn cells) and transiently co-transfected with the human dopamine transporter (hDAT) cDNA (SHα-Syn/hDAT cells) in the presence or absence of specific GSK-3β inhibitors. Results in part d) show cell viability, measured by the MTT reduction assay. Experimental design, figure arrangements, and statistical analysis ($n = 3$) were performed as described in Figure 3, except that $p \leq 0.01$ was chosen to denote statistical significance (*) by the Student's *t*-test analysis of the MTT assay results in part d) ($n = 3$).

treated) cells. Results are reported as the mean ± SD of three separate experiments.

Oxidative damage, which is a putative trigger of GSK-3β activation, might also be involved in the MPP^+-induced hyperphosphorylated Tau at the PHF-1 binding site. As shown in Figures 3c and 4c, the parkinsonism-related neurotoxin MPP^+ was able to increase the expression level of the active form of GSK-3β (phosphorylation of Tyr216[42] in mesencephalic neurons and in SHα-Syn/hDAT cells). Immunoblot analysis with the anti-GSK-3β phosphorylation-specific (pY216) antibody, which

recognizes phosphotyrosine forms of GSK-3β, revealed that the level of the active form of GSK-3β increased significantly in mesencephalic neurons (by 140%) and in SHα-Syn/hDAT cells (by 20%) after treatment with MPP^+, in comparison with vehicle-treated control cells (Figures 3c,d and 4c,d). Incubation with **18** and **22** (1 μM) significantly decreased (by more than 76 and 50%, respectively) GSK-3β phosphorylation observed in the primary mesencephalic neurons (Figures 3c,d and 4c,d). In SHα-Syn/hDAT, both inhibitors restored the quantity of the active form of GSK-3β to normal levels in this cellular model. Representative immunoblots are shown. Quantities obtained by the densitometry of blots probed with the antibodies raised against phosphorylated GSK-3β (pY216) were normalized with respect to the densitometric values determined with the total anti-GSK-3β antibody. Results represent the mean ±SD of three separate determinations.

MPP^+ leads to neuronal death through inhibition of the mitochondrial complex I which results in oxidative stress.[43] As active GSK-3β triggers signal transduction events which participate in cell death,[44,45] we suggest that blocking the expression of the active form of GSK-3β or blocking its activity by maleimides **18** and **22** may inhibit the MPP^+-induced decrease in the number of viable neuronal cells.

Primary cultures of mesencephalic neurons and SHα-Syn/hDAT cells were treated with MPP^+ (50 μM) for 48 h in the absence or presence of GSK-3β inhibitors. MPP^+ treatment caused a decrease in viability in mesencephalic neurons by 47% (Figure 3d) and in SHα-Syn/hDAT cells by 37% (Figure 4d), relative to the respective vehicle-treated controls. Treatment of both neurons and SHα-Syn/hDAT cells with maleimides **18** and **22** led to attenuated decreases in cell viability as assessed by the MTT assay, which were not significantly different than the number of viable cells found for the respective vehicle-treated control groups. Viability was assessed by the MTT assay. Values from each treatment are expressed as mean OD ±SD determined in triplicate from three independent cultures.

Conclusions

All the results presented herein support the hypothesis that MPP^+ is a neurotoxin that drives the phosphorylation of Tau by GSK-3β at the PHF-1 binding site. Furthermore, changes in the level of phosphorylated PHF-Tau are shown to be associated with increased α-Syn protein expression accompanied by decreases in cell viability. We have shown that the maleimides **18** and **22** inhibit Tau phosphorylation at a GSK-3β-specific site (Ser 396/404). Accordingly, compounds **18** and **22** may protect neuronal cells against cell death by decreasing the level of α-Syn protein expression. We conclude that the GSK-3β inhibitors described herein may be promising in defending cells against MPP^+-induced neurotoxicity, and that such compounds are valuable to explore in animal models of Parkinson's disease as well as in other Tau-related disease states. By using the SAR information presented herein in concert with broader screening assays performed to assess the inhibitory activity of these compounds toward other kinases together with data from animal studies, it is our plan to optimize the druglike character of these maleimides for use in neurodegenerative conditions.

Experimental Section

Synthesis: ^{1}H NMR and ^{13}C NMR spectra were recorded on a Bruker spectrometer at 360 and 75 MHz, respectively, with TMS as an internal standard. MS data were measured in the EI or ESI mode at an ionization potential of 70 eV; HRMS experiments were performed on a Q-TOF-2TM (Micromass). TLC was carried out with Merck 250 mm 60 F_{254} silica gel plates. Preparative TLC was performed with Analtech 1000 mm silica gel GF plates. Column chromatography was performed with Merck silica gel (40–60 mesh). Analytical HPLC was carried out on an Ace 5AQ column (25 cm × 4.6 mm), with detection at $\lambda = 254$ and 366 nm on a Shimadzu SPD-10A VP detector.

General procedure for maleimides 5–35: The following method represents a typical procedure for the synthesis of the 3-indolyl-4-indazolylmalemide-based ligands.

3-[5-Chloro-1-(2-methoxyethyl)-1*H*-indol-3-yl]-4-(1*H*-indazol-3-yl)-pyrrole-2,5-dione (17): NaH (55% suspension in mineral oil, 290 mg, 6.60 mmol) was added to a solution of 5-chloroindole (500 mg, 3.30 mmol) in dry DMF (6 mL) cooled with an ice bath, followed by 2-bromoethyl methyl ether (500 mg, 3.60 mmol), after which the reaction mixture was allowed to warm to room temperature. After 6 h, the reaction mixture was poured into ice water; HCl (1 N) was added to adjust the solution to ≈pH 4, and this was followed by extraction with ethyl acetate. The ethyl acetate extract was washed with water and brine, dried over anhydrous Na_2SO_4, and concentrated in vacuo. The residue was filtered through silica gel (ethyl acetate/hexane 1:4). The product was subjected to further reaction without additional purification. A solution of oxalyl chloride in THF (1.0 M, 6.60 mL) was added dropwise to a solution of 5-chloro-1-(2-methoxyethyl)-1*H*-indole in Et_2O (10 mL) cooled to 0 °C. The reaction was then stirred for 0.5 h at 0 °C, warmed to room temperature, and stirred overnight. It was then cooled to −60 °C, and a solution of NaOMe in MeOH (21%, 3.50 mL, 13.19 mmol) was added, after which the reaction mixture was allowed to warm to room temperature. The reaction was quenched by the addition of water and diluted with ethyl acetate. The organic layer was separated, dried over anhydrous Na_2SO_4, and concentrated. The residue was purified by column chromatography (ethyl acetate/hexane 1:3) to give the product (570 mg, 58%). ^{1}H NMR ($CDCl_3$, 360 MHz): $\delta = 3.28$ (s, 3H), 3.67 (t, $J = 5.4$ Hz, 2H), 3.94 (s, 3H), 4.24 (t, $J = 5.4$ Hz, 2H), 6.42 (d, $J = 2.9$ Hz, 1H), 7.13 (dd, $J = 2.0$, 8.2 Hz, 1H), 7.16 (d, $J = 2.9$ Hz, 1H), 7.25 (d, $J = 8.2$ Hz, 1H), 7.57 ppm (d, $J = 2.0$, 1H).

The indazolyl-3-acetamides **4** were prepared from 2-nitrobenzaldehyde and 5-chloro-2-nitrobenzaldehyde according to published procedures.[13,14] A solution of *t*BuOK in THF (1.0 M, 1.0 mL) was added dropwise to a suspension of indazolyl-3-acetamide (**4**: Y = H, R^2 = H; 42 mg, 0.24 mmol) and indolyl-3-glyoxylate (**3**: X = 5-Cl, R^1 = 3-methoxyethyl; 92 mg, 0.31 mmol) in dry THF (2.5 mL) at 0 °C, and the reaction mixture was allowed to stir at room temperature overnight. The reaction was quenched with HCl (12 N) and diluted with EtOAc. The organic solution was washed with saturated $NaHCO_3$, brine, then dried over Na_2SO_4, evaporated in vacuo, and purified by preparative TLC (MeOH/$CHCl_3$ 1:9) to afford product (53 mg, 53%) as an orange solid. ^{1}H NMR ([D_6]DMSO, 360 MHz): $\delta = 3.19$ (s, 3H), 3.63 (t, $J = 5.4$ Hz, 2H), 4.39 (t, $J = 5.4$ Hz, 2H), 6.20 (d, $J = 8.6$ Hz, 1H), 7.02–7.06 (m, 2H), 7.34 (t, $J = 7.2$ Hz, 1H), 7.50–

7.60 (m, 3H), 8.19 (s, 1H), 11.20 (s, 1H), 13.48 ppm (s, 1H); ^{13}C NMR ([D$_6$]DMSO, 75 MHz): δ = 46.8, 58.9, 71.4, 104.8, 111.1, 113.0, 121.3, 121.6, 122.0, 122.5, 123.1, 124.5, 125.5, 127.0, 127.1, 134.6, 125.7, 136.6, 141.4, 172.6, 172.9 ppm; FAB–HRMS calcd for $C_{22}H_{17}ClN_4O_3$ [M+Na]$^+$: 443.0887, found: 443.0872; HPLC purity: 96%.

3-(3-Indazolyl)-4-(3-indolyl)-1*H*-pyrrole-2,5-dione (5): ^{1}H NMR ([D$_6$]DMSO, 300 MHz): δ = 6.31 (d, J = 7.8 Hz, 1H), 6.60 (t, J = 7.2 Hz, 1H), 6.96–7.06 (m, 2H), 7.30–7.38 (m, 2H), 7.55 (d, J = 8.7 Hz, 1H), 8.12 (d, J = 3.0 Hz, 1H), 11.12 (s, 1H), 11.86 (s, 1H), 13.39 ppm (s, 1H); ^{13}C NMR ([D$_6$]DMSO, 75 MHz): δ = 105.3, 110.4, 112.1, 119.9, 120.8, 121.5, 122.0, 122.6, 123.1, 124.9, 126.3, 131.6, 134.9, 135.7, 136.5, 140.6, 172.2, 172.4 ppm; FAB–HRMS calcd for $C_{19}H_{12}N_4O_2$ [M+Na]$^+$: 351.0857, found: 351.0852; HPLC purity: 97%.

3-(3-Indazolyl)-4-[(1-methyl)-3-indolyl]-1*H*-pyrrole-2,5-dione (6): ^{1}H NMR ([D$_6$]DMSO, 360 MHz): δ = 3.88 (s, 3H), 6.21 (d, J = 8.1 Hz, 1H), 6.62 (t, J = 8.1 Hz, 1H), 7.02–7.08 (m, 2H), 7.34 (t, J = 8.1 Hz, 1H), 7.43 (d, J = 8.1 Hz, 1H), 7.54–7.59 (m, 2H), 8.45 (s, 1H), 11.14 (s, 1H), 13.38 ppm (s, 1H); ^{13}C NMR ([D$_6$]DMSO, 75 MHz): δ = 33.2, 104.3, 110.6, 120.3, 120.9, 121.5, 122.2, 125.3, 126.4, 135.3, 137.1, 172.2, 172.4 ppm; FAB–HRMS calcd for $C_{20}H_{14}N_4O_2$ [M+Na]$^+$: 365.1014, found: 365.1014; HPLC purity: 95%.

3-(3-1*H*-Indazol-3-yl)-4-[1-(3-trityloxypropyl)-1*H*-indol-3-yl]-pyrrole-2,5-dione (7): ^{1}H NMR ([D$_6$]DMSO, 360 MHz): δ = 1.80–1.95 (m, 2H), 3.4–3.43 (m, 2H), 4.33 (t, J = 6.9 Hz, 2H), 4.68 (t, J = 4.8 Hz, 1H), 6.29 (d, J = 8.1 Hz, 1H), 6.64 (t, J = 7.5 Hz, 1H), 7.05 (t, J = 8.1 Hz, 2H), 7.34 (t, J = 8.4 Hz, 1H), 7.48 (d, J = 8.4 Hz, 1H), 7.54–7.59 (m, 2H), 8.15 (s, 1H), 11.14 (s, 1H), 13.41 ppm (s, 1H); ^{13}C NMR ([D$_6$]DMSO, 75 MHz): δ = 32.8, 43.1, 57.7, 104.5, 110.4, 110.6, 120.2, 120.9, 121.1, 121.5, 122.1, 122.5, 125.4, 126.4, 134.5, 172.1, 172.4 ppm; FAB–HRMS calcd for $C_{41}H_{32}N_4O_3$ [M+Na]$^+$: 651.2372, found: 651.2386; HPLC purity: 98%.

3-(3-Indazolyl)-4-[1-(3-hydroxypropyl)-3-indolyl]-1*H*-pyrrole-2,5-dione (8): ^{1}H NMR ([D$_6$]DMSO, 360 MHz): δ = 1.80–1.95 (m, 2H), 3.4–3.43 (m, 2H), 4.33 (t, J = 6.9 Hz, 2H), 4.68 (t, J = 4.8 Hz, 1H), 6.29 (d, J = 8.1 Hz, 1H), 6.64 (t, J = 7.5 Hz, 1H), 7.05 (t, J = 8.1 Hz, 2H), 7.34 (t, J = 8.4 Hz, 1H), 7.48 (d, J = 8.4 Hz, 1H), 7.54–7.59 (m, 2H), 8.15 (s, 1H), 11.14 (s, 1H), 13.41 ppm (s, 1H); ^{13}C NMR ([D$_6$]DMSO, 75 MHz): δ = 32.8, 43.1, 57.7, 104.5, 110.4, 110.6, 120.2, 120.9, 121.1, 121.5, 122.1, 122.5, 125.4, 126.4, 134.5, 172.1, 172.4 ppm; FAB–HRMS calcd for $C_{22}H_{18}N_4O_3$ [M+Na]$^+$: 409.1276, found: 409.1270; HPLC purity: 96%.

3-(1*H*-Indazol-3-yl)-4-[1-(2-methoxyethyl)-1*H*-indol-3-yl]-pyrrole-2,5-dione (9): ^{1}H NMR ([D$_6$]DMSO, 360 MHz): δ = 3.21 (s, 3H), 3.65 (t, J = 5.0 Hz, 2H), 4.41 (t, J = 5.0 Hz, 2H), 6.28 (d, J = 7.9 Hz, 1H), 6.62 (t, J = 7.2 Hz, 1H), 7.00–7.05 (m, 2H), 7.33 (t, J = 7.2 Hz, 1H), 7.47–7.59 (m, 3H), 8.13 (s, 1H), 11.11 (s, 1H), 13.36 ppm (s, 1H); ^{13}C NMR ([D$_6$]DMSO, 75 MHz): δ = 46.8, 58.9, 71.4, 104.8, 111.1, 113.0, 121.3, 121.6, 122.0, 122.5, 123.1, 124.5, 125.5, 127.0, 127.1, 134.6, 125.7, 136.6, 141.4, 172.6, 172.9 ppm; FAB–HRMS calcd for $C_{22}H_{18}N_4O_3$ [M+Na]$^+$: 409.1285, found: 409.1276; HPLC purity: 95%.

3-(1-Methyl-1*H*-indazol-3-yl)-4-(1-methyl-1*H*-indol-3-yl)-pyrrole-2,5-dione (10): ^{1}H NMR ([D$_6$]DMSO, 360 MHz): δ = 3.90 (s, 3H), 3.98 (s, 3H), 6.20 (d, J = 7.5 Hz, 1H), 6.67 (t, J = 7.2 Hz, 1H), 7.06–7.11 (m, 2H), 7.37–7.46 (m, 2H), 7.57 (d, J = 8.4 Hz, 1H), 7.68 (d, J = 9.0 Hz, 1H), 8.20 (s, 1H), 11.15 ppm (s, 1H); ^{13}C NMR ([D$_6$]DMSO, 75 MHz): δ = 33.2, 35.8, 104.3, 110.0, 110.5, 120.0, 121.0, 121.3, 121.7, 122.2, 123.2, 125.2, 126.4, 134.5, 135.5, 137.0, 140.4, 172.1, 172.4 ppm; FAB–HRMS calcd for $C_{21}H_{16}N_4O_2$ [M+Na]$^+$: 379.1170, found: 379.1166; HPLC purity: 96%.

3-[1-(2-methoxyethyl)-1*H*-indazol-3-yl]-4-(1-methyl-1*H*-indol-3-yl)-pyrrole-2,5-dione (11): ^{1}H NMR ([D$_6$]DMSO, 360 MHz): δ = 3.14 (s, 3H), 3.51 (t, J = 5.0 Hz, 2H), 3.88 (s, 3H), 4.48 (t, J = 5.0 Hz, 2H), 6.24 (d, J = 7.9 Hz, 1H), 6.64 (t, J = 7.2 Hz, 1H), 7.04–7.09 (m, 2H), 7.35 (t, J = 7.2 Hz, 1H), 7.43 (d, J = 7.9 Hz, 1H), 7.59 (d, J = 8.2 Hz, 1H), 7.67 (d, J = 8.2 Hz, 1H), 8.20 (s, 1H), 11.13 ppm (s, 1H); ^{13}C NMR ([D$_6$]DMSO, 75 MHz): δ = 33.8, 49.0, 56.6, 71.3, 104.9, 111.0, 111.1, 120.9, 121.6, 121.9, 122.4, 122.7, 122.8, 123.8, 125.8, 127.0, 135.1, 135.6, 136.2, 141.3, 172.8, 173.0 ppm; FAB–HRMS calcd for $C_{23}H_{20}N_4O_3$ [M+Na]$^+$: 423.1433, found: 423.1432; HPLC purity: 96%.

3-[4-(1*H*-indazol-3-yl)-2,5-dioxo-2,5-dihydro-1*H*-pyrrol-3-yl]-1-methyl-1*H*-indole-5-carbonitrile (12): ^{1}H NMR ([D$_6$]DMSO, 360 MHz): δ = 6.75 (s, 1H), 7.05 (t, J = 4.9 Hz, 1H), 7.31–7.42 (m, 2H), 7.53–7.60 (m, 3H), 8.28 (s, 1H), 12.34 (s, 1H), 13.57 ppm (s, 1H); ^{13}C NMR ([D$_6$]DMSO, 75 MHz): δ = 102.3, 106.0, 110.7, 113.8, 120.3, 121.3, 121.6, 122.6, 124.9, 125.0, 125.5, 126.7, 126.8, 133.8, 134.1, 135.5, 138.6, 141.0, 172.1, 172.4 ppm; FAB–HRMS calcd for $C_{20}H_{11}N_5O_2$ [M+Na]$^+$: 376.0811, found: 376.0801; HPLC purity: 95%.

3-(1*H*-Indazol-3-yl)-4-(1-methyl-5-nitro-1*H*-indol-3-yl)-pyrrole-2,5-dione (13): ^{1}H NMR (MeOD, 360 MHz): δ = 3.32 (s, 3H), 7.05 (t, J = 6.9 Hz, 1H), 7.21 (d, J = 2.0 Hz, 1H), 7.34 (t, J = 6.9 Hz, 1H), 7.57 (m, 2H), 7.66 (d, J = 9.1 Hz, 1H), 7.95 (dd, J = 9.1, 2.0 Hz, 1H), 8.37 (s, 1H), 11.29 (s, 1H), 13.50 ppm (s, 1H); ^{13}C NMR (MeOD, 75 MHz): δ = 34.3, 107.0, 111.2, 111.9, 117.7, 118.9, 121.75, 122.0, 123.0, 125.2, 126.0, 127.17, 133.5, 135.8, 138.8, 141.5, 141.7, 172.4, 172.7 ppm; FAB–HRMS calcd for $C_{20}H_{13}N_5O_4$ [M+Na]$^+$: 410.0865, found: 410.0862; HPLC purity: 97%.

3-(1*H*-Indazol-3-yl)-4-[1-(2-methoxyethyl)-5-nitro-1*H*-indol-3-yl]-pyrrole-2,5-dione (14): ^{1}H NMR (MeOD, 360 MHz): δ = 3.97 (s, 3H), 3.74 (t, J = 5.0 Hz, 2H), 4.47 (t, J = 5.0 Hz, 1H), 6.93 (t, J = 7.9 Hz, 1H), 7.16 (d, J = 2.1 Hz, 1H), 7.28–7.36 (m, 2H), 7.53 (d, J = 8.2 Hz, 1H), 7.56 (d, J = 9.0 Hz, 1H), 7.90 (d, J = 9.0 Hz, 1H), 8.31 ppm (s, 1H); ^{13}C NMR (MeOD, 75 MHz): δ = 47.0, 58.1, 71.2, 107.1, 110.5, 110.7, 117.2, 118.2, 120.9, 121.3, 122.7, 125.2, 126.9, 137.59, 140.0, 141.95, 172.2 ppm; FAB–HRMS calcd for $C_{22}H_{17}N_5O_5$ [M+Na]$^+$: 454.1127, found: 454.1124; HPLC purity: 96%.

3-(5-Chloro-1-methyl-1*H*-indol-3-yl)-4-(1*H*-indazol-3-yl)-pyrrole-2,5-dione (15): ^{1}H NMR ([D$_6$]DMSO, 360 MHz): δ = 3.87 (s, 3H), 6.19 (d, J = 8.0 Hz, 1H), 6.65 (t, J = 7.2 Hz, 1H), 7.06 (t, J = 7.2 Hz, 1H), 7.35 (dd, J = 1.8, 8.8 Hz, 1H), 7.44 (d, J = 8.0 Hz, 1H), 7.59 (d, J = 8.8 Hz, 1H), 7.70 (d, J = 1.8 Hz, 1H), 8.13 (s, 1H), 11.14 (s, 1H), 13.53 ppm (s, 1H); ^{13}C NMR ([D$_6$]DMSO, 75 MHz): δ = 33.8, 104.8, 111.2, 112.9, 120.9, 121.5, 121.6, 122.8, 122.9, 124.0, 125.8, 125.9, 127.4, 135.2, 136.0, 136.2, 137.8, 139.9, 172.8, 173.0 ppm; FAB–HRMS calcd for $C_{20}H_{13}ClN_4O_2$ [M+Na]$^+$: 399.0624, found: 399.0618; HPLC purity: 97%.

3-[5-Chloro-1-(3-hydroxypropyl)-1*H*-indol-3-yl]-4-(1*H*-indazol-3-yl)-pyrrole-2,5-dione (16): ^{1}H NMR ([D$_6$]DMSO, 360 MHz): δ = 1.87 (m, 2H), 3.34 (t, J = 6.8 Hz, 2H), 4.30 (t, J = 6.8 Hz, 2H), 4.66 (br s, 1H), 6.31 (d, J = 8.6 Hz, 1H), 6.70 (dd, J = 1.8, 8.6 Hz, 1H), 7.02 (t, J = 7.9 Hz, 1H), 7.32 (t, J = 7.9 Hz, 1H), 7.54 (d, J = 8.6 Hz, 2H), 8.13 (s, 1H), 11.15 (s, 1H), 13.43 ppm (s, 1H); ^{13}C NMR ([D$_6$]DMSO, 75 MHz): δ = 33.4, 43.8, 58.3, 106.3, 111.2, 120.9, 121.6, 122.2, 123.0, 123.1, 124.8, 124.9, 127.0, 127.6, 134.3, 135.8, 136.0, 137.5, 141.4, 172.8, 173.0 ppm; FAB–HRMS calcd for $C_{22}H_{17}ClN_4O_3$ [M+Na]$^+$: 443.0887, found: 443.0887; HPLC purity: 95%.

3-(5-Flouro-1*H*-indol-3-yl)-4-(1*H*-indazol-3-yl)-pyrrole-2,5-dione (18): ^{1}H NMR ([D$_6$]DMSO, 400 MHz): δ = 5.93 (dd, J = 2.0, 11.2 Hz, 1H), 6.85 (ddd, J = 2.0, 9.0, 11.2 Hz, 1H), 7.02 (t, J = 8.0 Hz, 1H),

7.33–7.39 (m, 2H), 7.55–7.59 (m, 2H), 8.19 (s, 1H), 11.16 (s, 1H), 11.98 (s, 1H), 13.48 ppm (s, 1H); ^{13}C NMR ([D$_6$]DMSO, 75 MHz): δ = 105.6, 105.7, 106.1, 106.3, 110.3, 110.6, 110.7, 113.3, 113.4, 121.2, 121.7, 122.8, 123.6, 125.7, 125.8, 126.7, 133.4, 133.5, 134.9, 135.9, 140.9, 156.1, 158.4, 172.3, 172.6 ppm; FAB–HRMS calcd for $C_{19}H_{11}FN_4O_2$ [*M*+H]$^+$: 347.0944, found: 347.0952; HPLC purity: 97%.

3-(5-Flouro-1-methyl-1*H*-indol-3-yl)-4-(1*H*-indazol-3-yl)-pyrrole-2,5-dione (19): ^{1}H NMR ([D$_6$]DMSO, 400 MHz): δ = 3.88 (s, 3H), 5.87 (dd, *J* = 2.4, 9.0 Hz, 1H), 6.92 (td, *J* = 2.0, 9.0 Hz, 1H), 7.06 (t, *J* = 7.6 Hz, 1H), 7.36 (t, *J* = 7.6 Hz, 1H), 7.45 (dd, *J* = 4.5, 9.0 Hz, 1H), 7.58 (m, 2H), 8.22 (s, 1H), 11.15 (s, 1H), 13.47 ppm (s, 1H); ^{13}C NMR ([D$_6$]DMSO, 75 MHz): δ = 31.7, 105.6, 105.7, 106.1, 106.3, 110.3, 110.6, 110.7, 113.3, 113.4, 121.2, 121.7, 122.8, 123.6, 125.7, 125.8, 126.7, 133.4, 133.5, 134.9, 135.9, 140.9, 156.1, 158.4, 172.3, 172.6 ppm; FAB–HRMS calcd for $C_{20}H_{13}FN_4O_2$ [*M*+Na]$^+$: 383.0921, found: 383.0923; HPLC purity: 96%.

3-[5-Fluoro-1-(2-methoxy-ethyl)-1*H*-indol-3-yl]-4-(1*H*-indazol-3-yl)-pyrrole-2,5-dione (20): ^{1}H NMR ([D$_6$]DMSO, 360 MHz): δ = 3.36 (s, 3H), 3.65 (t, *J* = 5.0 Hz, 2H), 4.42 (t, *J* = 5.0 Hz, 2H), 5.91 (dd, *J* = 2.5, 9.0 Hz, 1H), 6.91 (td, *J* = 2.5, 9.0 Hz, 1H), 7.06 (t, *J* = 7.5 Hz, 1H), 7.35 (t, *J* = 7.5 Hz, 1H), 7.51 (q, *J* = 9.0 Hz, 1H), 7.56–7.59 (m, 2H), 8.21 (s, 1H), 11.16 (s, 1H), 13.45 ppm (s, 1H); ^{13}C NMR ([D$_6$]DMSO, 75 MHz): δ = 46.9, 58.9, 71.4, 105.2, 105.3, 106.7, 107.0, 110.6, 110.9, 111.1, 112.5, 112.6, 121.6, 122.1, 123.1, 124.0, 126.4, 126.5, 127.1, 133.9, 134.7, 136.2, 136.9, 141.3, 156.5, 159.1, 172.7, 172.9 ppm; FAB–HRMS calcd for $C_{22}H_{17}FN_4O_3$ [*M*+Na]$^+$: 427.1182, found: 427.1183; HPLC purity: 97%.

3-(5-Bromo-1*H*-indol-3-yl)-4-(1*H*-indazol-3-yl)-pyrrole-2,5-dione (21): ^{1}H NMR ([D$_6$]DMSO, 400 MHz): δ = 6.36 (d, *J* = 1.4 Hz, 1H), 7.05 (t, *J* = 7.5 Hz, 1H), 6.11 (dd, *J* = 1.5, 8.5 Hz, 1H), 7.33–7.37 (m, 2H), 7.55 (d, *J* = 8.5 Hz, 1H), 7.58 (d, *J* = 8.5 Hz, 1H), 8.17 (s, 1H), 11.16 (s, 1H), 12.02 (s, 1H), 13.50 ppm (s, 1H); ^{13}C NMR ([D$_6$]DMSO, 75 MHz): δ = 105.1, 110.7, 112.9, 114.2, 121.2, 121.5, 122.8, 123.8, 124.1, 124.7, 126.7, 126.9, 133.0, 134.8, 135.4, 135.8, 141.0, 172.3, 172.5 ppm; FAB–HRMS calcd for $C_{19}H_{11}BrN_4O_2$ [*M*+Na]$^+$: 428.9963, found: 428.9955; HPLC purity: 98%.

3-(5-Bromo-1-methyl-1*H*-indol-3-yl)-4-(1*H*-indazol-3-yl)-pyrrole-2,5-dione (22): ^{1}H NMR ([D$_6$]DMSO, 400 MHz): δ = 3.87 (s, 3H), 6.25 (d, *J* = 1.4 Hz, 1H), 7.06 (t, *J* = 7.2 Hz, 1H), 7.17 (dd, *J* = 1.4, 8.6 Hz, 1H), 7.36 (t, *J* = 7.2 Hz, 1H), 7.42 (d, *J* = 8.6 Hz, 1H), 7.58 (m, 2H), 8.20 (s, 1H), 11.18 (s, 1H), 13.49 ppm (s, 1H); ^{13}C NMR ([D$_6$]DMSO, 75 MHz): δ = 33.6, 104.1, 110.7, 112.8, 113.3, 121.2, 121.5, 122.9, 123.9, 124.0, 124.7, 126.6, 127.2, 134.3, 135.8, 136.0, 136.6, 141.0, 172.3, 172.5 ppm; FAB–HRMS calcd for $C_{20}H_{13}BrN_4O_2$ [*M*+Na]$^+$: 443.0120, found: 443.0126; HPLC purity: 97%.

3-(5-Chloro-1*H*-indazol-3-yl)-4-[5-fluoro-1-(2-methoxyethyl)-1*H*-indol-3-yl]-pyrrole-2,5-dione (23): ^{1}H NMR (MeOD, 360 MHz): δ = 3.32 (s, 3H), 3.74 (t, *J* = 5.0 Hz, 2H), 4.33 (t, *J* = 5.0 Hz, 2H), 5.99 (dd, *J* = 2.5, 9.0 Hz, 1H), 6.82 (td, *J* = 2.5, 9.0 Hz, 1H), 7.22–7.27 (m, 2H), 7.35 (dd, *J* = 0.7, 1.8 Hz, 1H), 7.46 (dd, *J* = 0.7, 9.0 Hz, 1H), 8.11 ppm (s, 1H); ^{13}C NMR (MeOD), 75 MHz): δ = 47.0, 59.0, 71.0, 105.0, 105.1, 106.7, 107.0, 110.6, 110.7, 111.0, 111.6, 119.7, 120.6, 122.2, 123.4, 126.2, 126.3, 126.9, 127.4, 133.2, 134.5, 135.3, 135.8, 139.4, 156.3, 159.3, 171.7, 171.9 ppm; FAB–HRMS calcd for $C_{22}H_{16}ClFN_4O_3$ [*M*+Na]$^+$: 461.0792, found: 461.0790; HPLC purity: 96%.

3-(5-Benzyloxy-1-methyl-1*H*-indol-3-yl)-4-(1*H*-indazol-3-yl)-pyrrole-2,5-dione (24): ^{1}H NMR ([D$_6$]DMSO, 360 MHz): δ = 3.88 (s, 3H), 3.94 (s, 2H), 5.58 (d, *J* = 2.4 Hz, 1H), 6.73 (dd, *J* = 8.7, 2.4 Hz, 1H), 7.06–7.15 (m, 3H), 7.23–7.39 (m, 5H), 7.59 (d, *J* = 8.1 Hz, 1H), 7.69 (d, *J* = 8.4 Hz, 1H), 8.14 (s, 1H), 11.12 (s, 1H), 13.43 ppm (s, 1H); FAB–HRMS calcd for $C_{27}H_{20}N_4O_3$ [*M*+Na]$^+$: 471.1433, found: 471.1421; HPLC purity: 97%.

3-[5-Benzyloxy-1-(3-hydroxypropyl)-1*H*-indole-3-yl]-4-(1*H*-indazol-3-yl)-pyrrole-2,5-dione (25): ^{1}H NMR (MeOD, 360 MHz): δ = 2.06 (m, 2H), 3.58 (t, *J* = 6.8 Hz, 2H), 3.94 (s, 2H), 4.34 (t, *J* = 6.8 Hz, 2H), 5.69 (s, 1H), 6.70 (dd, *J* = 2.4, 8.6 Hz, 1H), 7.03–7.11 (m, 3H), 7.23–7.38 (m, 5H), 7.52–7.57 (m, 2H), 8.13 ppm (s, 1H); ^{13}C NMR (MeOD, 75 MHz): δ = 32.7, 43.4, 58.4, 69.4, 104.0, 105.0, 111.0, 113.5, 121.3, 121.6, 123.3, 126.5, 127.2, 127.3, 127.6, 128.2, 132.1, 134.9, 135.9, 137.4, 153.9, 172.8, 172.9 ppm; FAB–HRMS calcd for $C_{29}H_{24}N_4O_4$ [*M*+Na]$^+$: 515.1695, found: 515.1704; HPLC purity: 98%.

3-[5-Benzyloxy-1-(2-methoxyethyl)-1*H*-indole-3-yl]-4-(1*H*-indazol-3-yl)-pyrrole-2,5-dione (26): ^{1}H NMR ([D$_6$]DMSO, 360 MHz): δ = 3.11 (s, 3H), 3.65 (t, *J* = 5.0 Hz, 2H), 3.91 (s, 2H), 4.39 (t, *J* = 5.0 Hz, 1H), 6.68 (dd, *J* = 2.5, 9.0 Hz, 1H), 7.02–7.04 (m, 2H), 7.09–7.13 (m, 2H), 7.22–7.40 (m, 6H), 7.56 (d, *J* = 8.4 Hz, 1H), 7.68 (d, *J* = 8.2 Hz, 1H), 8.11 (s, 1H), 11.10 (s, 1H), 13.41 ppm (s, 1H); ^{13}C NMR ([D$_6$]DMSO, 75 MHz): δ = 46.8, 58.9, 69.1, 71.5, 104.5, 105.0, 121.6, 122.2, 122.5, 123.5, 127.2, 128.0, 128.2, 128.7, 128.8, 129.0, 132.3, 135.4, 135.8, 137.5, 141.5, 153.5, 172.9, 173.0 ppm; FAB–HRMS calcd for $C_{29}H_{24}N_4O_4$ [*M*+Na]$^+$: 515.1695, found: 515.1700; HPLC purity: 98%.

3-[5-Benzyloxy-1-(3-methoxyethyl)-1*H*-indole-3-yl]-4-(5-chloro-1*H*-indazol-3-yl)-pyrrole-2,5-dione (27): ^{1}H NMR (MeOD, 360 MHz): δ = 3.32 (s, 3H), 3.74 (t, *J* = 5.0 Hz, 2H), 4.06 (s, 2H), 4.38 (t, *J* = 5.0 Hz, 2H), 5.68 (d, *J* = 2.3, 1H), 6.73 (dd, *J* = 2.3, 8.6 Hz, 1H), 7.08–7.21 (m, 2H), 7.22–7.33 (m, 5H), 7.50–7.53 (m, 2H), 8.13 ppm (s, 1H); ^{13}C NMR (MeOD, 75 MHz): δ = 58.2, 69.5, 71.3, 104.0, 104.9, 111.1, 111.6, 113.5, 120.9, 127.1, 127.6, 127.7, 128.2, 132.3, 135.5, 137.3, 153.9, 172.6, 172.7 ppm; FAB–HRMS calcd for $C_{29}H_{23}N_4O_4$ [*M*+Na]$^+$: 549.1306, found: 549.1309; HPLC purity: 96%.

3-(1*H*-Indazol-3-yl)-4-(1-methyl-6-nitro-1*H*-indol-3-yl)-pyrrole-2,5-dione (28): ^{1}H NMR (MeOD, 360 MHz): δ = 4.00 (s, 3H), 6.50 (d, *J* = 9.0 Hz, 1H), 7.05 (t, *J* = 7.9 Hz, 1H), 7.33 (t, *J* = 7.9 Hz, 1H), 7.48–7.57 (m, 2H), 7.62 (d, *J* = 8.3 Hz, 1H), 8.41 (s, 1H), 8.45 ppm (s, 1H); ^{13}C NMR (MeOD, 75 MHz): δ = 34.3, 105.6, 108.3, 111.2, 115.4, 121.8, 121.9, 122.3, 122.9, 126.6, 127.1, 130.7, 133.4, 135.8, 136.3, 140.8, 141.4, 143.0, 172.7, 172.9 ppm; FAB–HRMS calcd for $C_{20}H_{13}N_5O_4$ [*M*+Na]$^+$: 410.0865, found: 410.0865; HPLC purity: 97%.

3-(6-Chloro-1-methyl-1*H*-indol-3-yl)-4-(1*H*-indazol-3-yl)-pyrrole-2,5-dione (29): ^{1}H NMR (MeOD, 360 MHz): δ = 3.82 (s, 3H), 6.12 (d, *J* = 8.6 Hz, 1H), 6.51 (dd, *J* = 1.8, 8.6 Hz, 1H), 6.96 (t, *J* = 7.5 Hz, 1H), 7.31–7.40 (m, 3H), 7.53 (d, *J* = 8.6 Hz, 1H), 8.04 ppm (s, 1H); ^{13}C NMR (MeOD, 75 MHz): δ = 32.5, 105.1, 110.0, 110.2, 120.6, 121.2, 121.3, 122.1, 124.5, 127.0, 128.3, 136.0, 138.2, 172.0, 172.1 ppm; FAB–HRMS calcd for $C_{20}H_{13}ClN_4O_2$ [*M*+Na]$^+$: 399.0625, found: 399.0627; HPLC purity: 96%.

3-(6-Flouro-1*H*-indol-3-yl)-4-(1*H*-indazol-3-yl)-pyrrole-2,5-dione (30): ^{1}H NMR ([D$_6$]DMSO, 360 MHz): δ = 6.31 (dd, *J* = 4.1, 6.8 Hz, 1H), 6.50 (ddd, *J* = 1.8, 7.2, 8.8 Hz, 1H), 7.02 (t, *J* = 5.6 Hz, 1H), 7.16 (dd, *J* = 1.8, 7.2 Hz, 1H), 7.32 (t, *J* = 5.6 Hz, 1H), 7.54 (m, 2H), 8.09 (s, 1H), 11.14 (s, 1H), 11.88 (s, 1H), 13.42 ppm (s, 1H); ^{13}C NMR ([D$_6$]DMSO, 75 MHz): δ = 98.3, 98.6, 105.6, 108.4, 108.7, 110.7, 121.2, 121.8, 121.9, 123.1, 124.1, 126.6, 132.4, 134.7, 135.8, 136.7, 136.8, 140.9, 172.3, 172.6 ppm; FAB–HRMS calcd for $C_{19}H_{11}FN_4O_2$ [*M*+Na]$^+$: 369.0764, found: 369.0774; HPLC purity: 95%.

3-(5-Chloro-1*H*-indazol-3-yl)-4-[1-(2-methoxyethyl)-6-methyl-1*H*-indol-3-yl]-pyrrole-2,5-dione (31): ^{1}H NMR (MeOD, 360 MHz): δ =

2.30 (s, 1H), 3.31 (s, 3H), 3.71 (t, J=5.4 Hz, 2H), 4.26 (t, J=5.4 Hz, 2H), 6.27 (d, J=8.2 Hz, 1H), 6.51 (d, J=8.2 Hz, 1H), 7.05 (s, 1H), 7.21 (dd, J=1.6, 9.0 Hz, 1H), 7.36 (d, J=1.6 Hz, 1H), 7.43 (d, J=9.0 Hz, 1H), 8.00 (s, 1H), 8.51 ppm (br s, 1H); ^{13}C NMR (MeOD, 75 MHz): δ=22.0, 47.0, 59.4, 71.2, 105.4, 110.1, 110.2, 112.1, 121.3, 123.6, 123.7, 123.9, 127.3, 127.6, 128.0, 133.1, 134.8, 137.5, 139.7, 171.3, 171.4 ppm; FAB–HRMS calcd for $C_{23}H_{19}ClN_4O_3$ $[M+Na]^+$: 457.1043, found: 457.1057; HPLC purity: 97%.

3-[6-Benzyloxy-1-(2-methoxyethyl)-1*H*-indole-3-yl]-4-(1*H*-indazol-3-yl)-pyrrole-2,5-dione (32): ^{1}H NMR (MeOD, 360 MHz): δ=3.28 (s, 3H), 3.69 (t, J=5.4 Hz, 2H), 4.32 (t, J=5.4 Hz, 2H), 5.01 (s, 2H), 6.10 (d, J=8.6 Hz, 1H), 6.31 (dd, J=2.1, 8.6 Hz, 1H), 6.95 (t, J=7.5 Hz, 1H), 6.97 (d, J=2.1 Hz, 1H), 7.25–7.39 (m, 7H), 7.53 (d, J=8.6 Hz, 1H), 8.01 ppm (s, 1H); ^{13}C NMR (MeOD, 75 MHz): δ=46.7, 58.8, 67.9, 71.5, 104.3, 106.0, 121.6, 122.4, 122.5, 123.2, 127.5, 128.0, 128.2, 128.6, 128.8, 129.0, 132.6, 135.4,135.8, 138.0, 141.5, 153.7, 172.8, 172.9 ppm; FAB–HRMS calcd for $C_{29}H_{24}N_4O_4$ $[M+Na]^+$: 515.1695, found: 515.1690; HPLC purity: 98%.

3-[7-Benzyloxy-1-(2-methoxyethyl)-1*H*-indole-3-yl]-4-(1*H*-indazol-3-yl)-pyrrole-2,5-dione (33): ^{1}H NMR (MeOD, 360 MHz): δ=3.29 (s, 3H), 3.62 (t, J=5.4 Hz, 2H), 4.58 (t, J=5.4 Hz, 2H), 5.13 (s, 2H), 5.90 (d, J=7.8 Hz, 1H), 6.47 (t, J=7.8 Hz, 1H), 6.64 (d, J=7.8 Hz, 1H), 7.28–7.52 (m, 8H), 7.92 ppm (s, 1H); ^{13}C NMR (MeOD, 75 MHz): δ=42.5, 58.6, 70.0, 105.0, 105.9, 111.0, 113.7, 121.1, 121.6, 123.3, 126.0, 127.2, 127.3, 128.0, 128.2, 132.1, 135.0, 135.9, 137.6, 153.2, 172.7, 172.8 ppm; FAB–HRMS calcd for $C_{29}H_{24}N_4O_4$ $[M+H]^+$: 493.1876, found: 493.1882; HPLC purity: 98%.

3-(5-Chloro-1*H*-indazol-3-yl)-4-(1-methyl-1*H*-indol-3-yl)-pyrrole-2,5-dione (34): ^{1}H NMR ([D$_6$]DMSO, 360 MHz): δ=3.87 (s, 3H), 6.29 (d, J=8.0 Hz, 1H), 6.65 (t, J=7.2 Hz, 1H), 7.06 (t, J=7.2 Hz, 1H), 7.35 (dd, J=1.9, 8.6 Hz, 1H), 7.44 (d, J=8.0 Hz, 1H), 7.59 (d, J=8.8 Hz, 1H), 7.70 (d, J=1.9 Hz, 1H), 8.13 (s, 1H), 11.14 (s, 1H), 13.53 ppm (s, 1H); ^{13}C NMR ([D$_6$]DMSO, 75 MHz): δ=33.8, 104.8, 111.2, 112.9, 120.9, 121.5, 121.6, 122.8, 122.9, 124.0, 125.8, 125.9, 127.4, 135.3, 136.0, 136.2, 137.8, 139.9, 172.8, 173.0 ppm; FAB–HRMS calcd for $C_{20}H_{13}ClN_4O_2$ $[M+Na]^+$: 399.0625, found: 399.0631; HPLC purity: 96%.

3-(5-Chloro-1*H*-indazol-3-yl)-4-[1-(3-hydroxypropyl)-1*H*-indol-3-yl]-pyrrole-2,5-dione (35): ^{1}H NMR ([D$_6$]DMSO, 360 MHz): δ=1.80 (m, 2H), 3.39 (m, 2H), 4.32 (m, 2H), 6.25 (d, J=8.0 Hz, 1H), 6.64 (t, J=7.5 Hz, 1H), 7.04 (t, J=7.5 Hz, 1H), 7.33 (d, J=8.6 Hz, 1H), 7.48 (d, J=8.0 Hz, 2H), 7.56–7.61 (m, 2H), 8.13 (s, 1H), 11.14 (s, 1H), 13.56 ppm (s, 1H); ^{13}C NMR ([D$_6$]DMSO, 75 MHz): δ=33.5, 43.7, 58.35, 105.0, 111.3, 112.9, 120.9, 121.5, 121.7, 122.8, 123.1, 124.0, 125.9, 126.0, 127.3, 135.2, 136.2, 137.0, 139.8, 172.7, 172.9 ppm; FAB–HRMS calcd for $C_{22}H_{17}ClN_4O_3$ $[M+Na]^+$: 443.0887, found: 443.0903; HPLC purity: 97%.

Cloning and purification of GSK-3β: The cDNA for human GSK-3β was obtained from Dr. J. R. Woodgett (University of Toronto, Ontario, Canada) and subcloned into the pET29b vector (Novagen, Madison, WI, USA). The protein (His$_6$-GSK-3β/pET29b) was purified on a His-Select Nickel agarose column as described by the manufacturer (Sigma, St. Louis, MO, USA). As an alternate source, His$_6$-GSK-3β was purchased from EMD Biosciences/Calbiochem (Madison, WI, USA).

Kinase assays: Kinase assays were performed essentially as described by Welsh and co-workers.[46] GSK-3β activity was measured as the ability to transfer γ-^{32}P from [γ-^{32}P]ATP to the primed glycogen synthase peptide substrate (RRRPASVPPSPSLSRHS***S***HQRR, in which ***S*** denotes the designated primed phosphoserine residue). The ability of recombinant human His$_6$-GSK-3β (His$_6$-GSK-3β/pET29b, 4–53 nM, or 21 nM, EMD Biosciences) to phosphorylate the pGSM peptide substrate (10 μM final concentration) was assayed in the presence of ATP (10 or 100 μM, specific activity: 1.3 μCi [γ-^{32}P]ATP nM^{-1}). After incubation for 30 min at 30 °C, samples (25 μL volumes) were spotted on P81 Whatman filters (2.5 cm), dried for 30 s, and immediately transferred into a beaker containing 0.75% phosphoric acid. The filters were dried and counted in ScintiSafe cocktail (3 mL, Fisher Scientific, Hanover Park, IL, USA) in a Beckman LS6000IC scintillation counter (Beckman Coulter, Fullerton, CA, USA).

Docking: All molecular modeling studies were performed on an SGI or a Linux computer with the SYBYL 7.0[47] and CHARMM[48] (version 31) software packages. The coordinates for the kinase domain of GSK-3β were extracted from the co-crystal structure data of the complex between GSK-3β and staurosporine (PDB code: 1Q3D). The backbone atoms were fixed, and the complex was subjected to a short MD relaxation of the side chains followed by energy minimization using CHARMM. The resulting model of GSK-3β was examined by using the PROCHECK[49,50] program to verify its stereochemical quality. The stereochemical quality of the protein was similar to that of the starting protein. The active site was designated to consist of the amino acid residues within a radius of 6.5 Å from the original ligand. Val 135, Asp 133, Leu 132, Lys 85, Glu 97, and Arg 141 were set as a core subpocket. The following FlexX-Pharm settings were used to restrict the binding of the ligands to the ATP-binding site of GSK: Asp 133 is an optional acceptor, Val 135 is an optional donor, and a minimum of one optional criterion has to be satisfied.

A total of 95 GSK-3β ligands and their biological activity data were collected from several publications[6,7,51–58] and used for verifying the in silico docking and scoring methods. After ligand docking was performed by the FlexX and Flex-Pharm modules in SYBYL, the 30 best poses were selected for each ligand and saved for analysis by CScore. The Flex-Pharm method was used to restrict the docking of the ligands to the ATP-binding site. We used a combination of several functions and the criterion of consensus $\geq$3 to select the best pose for each ligand.[59–61] The binding modes of the docked ligands were found to be consistent with those expected for compounds that are structurally related to staurosporine and I-5.[56] Overall, the selection of the poses using Gold score and FlexX score, and scoring of the poses using the Chem score scoring function performed better than other docking/scoring functions available in CScore (Figure 5, correlation coefficient = 0.69). Therefore, the combination of these functions was used for further docking experiments[62] (see Table 2).

Cell culture and transfection: Human neuroblastoma SHSY5Y cells stably transfected with human wild-type α-Syn cDNA (SHα-Syn) were grown in DMEM/F12 medium containing FBS (10%), L-glutamine (2 mM), penicillin (100 U mL^{-1}), and streptomycin (100 μg mL^{-1}). Cells were transiently transfected with human dopamine transporter (hDAT; 2 μg DNA per 1.0×10^5 cells for 12-well dishes, and 4 μg DNA per 1.2×10^6 cells for 6-well dishes) at 80% confluency by the Lipofectamine reagent, accordingly to the manufacturer's protocol (Invitrogen). Cells were grown for a further 48 h after transfection to allow expression of the transgenes.

Primary mesencephalic neuronal cultures were prepared from the ventral mesencephalon of gestational 16–18-day-old rat embryos, and grown in Neurobasal medium (Invitrogen) supplemented with B27 Supplement (2% *v/v*, Invitrogen), a mixture of penicillin/streptomycin (10 U mL^{-1}), and 25 μM β-mercaptoethanol at 37 °C and 5% CO_2.

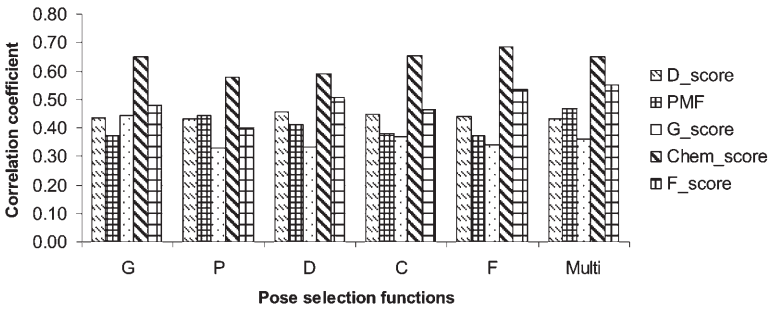

Figure 5. The Pearson correlation coefficient.

Table 2. Pearson product moment correlation coefficients between the docking scores and the experimental pIC_{50} values.

Pose Selection Function	Scoring Functions					
	Dock	PMF	Gold	Chem score	FlexX	Average
Gold	0.44	0.37	0.44	0.65	0.48	0.48
PMF	0.43	0.44	0.33	0.58	0.40	0.44
Dock	0.46	0.41	0.33	0.59	0.51	0.46
Chem score	0.45	0.38	0.37	0.65	0.46	0.46
FlexX	0.44	0.37	0.34	0.69	0.53	0.47
Multi[a]	0.43	0.47	0.36	0.65	0.55	0.49
Average	0.44	0.41	0.36	0.63	0.49	

[a] Gold:PMF:Dock:Chem score:FlexX = 1:1:1:1:1.

Cell treatment: MPP^+ iodide was prepared at a concentration of 50 μM and then added directly to the medium in the 6- or 12-well dishes. Cells were exposed to MPP^+ for 48 h. Concentrated stock solutions of the synthesized GSK-3β inhibitors **14**, **16**, **8**, **19**, **18**, and **22** were prepared in DMSO at a concentration of 10 mM. On the day of each experiment, each inhibitor was added to the wells to a final concentration of 1 μM. GSK-3β inhibitors were applied for the last 16 h of MPP^+ treatment.

Sample preparation and immunoblot analysis: Owing to different biochemical properties of the proteins analyzed, two separate protocols were used to check protein expression levels of α-Syn and GSK-3β (protocol I) and the phosphorylation pattern of Tau (protocol II) by Western blot.

Protocol I: Tissue or cells were collected by gentle scraping, were washed three times with DPBS, and lysed in buffer (50 mM Tris–HCl, pH 7.5, 150 mM NaCl, 1 mM EDTA) containing 0.1% Nonidet P-40, 0.1% Triton X-100, 1 mM phenylmethylsulfonyl fluoride, and protease inhibitor cocktail tablets (Complete Mini, EDTA-free, Roche Diagnostics GmbH, Germany). The cellular material was left for 20 min on ice. The lysate was then centrifuged for 10 min at 14000 *g*, and the supernatant was collected. Protein concentrations were measured with the Bradford assay (Bio-Rad, Richmond, CA, USA).

Protocol II: Cells were washed twice with ice-cold PBS and collected with 200 μL 2× stop solution (500 mM Tris–HCl, pH 6.8, 10% sodium dodecyl sulfate (SDS), 100 mM EDTA, 100 mM EGTA, 10% glycerol) containing a protease inhibitor mixture and the phosphatase inhibitor sodium orthovanadate (1 mM). Samples were sonicated, and protein concentrations were determined with the DC Protein assay (Bio-Rad, Richmond, CA, USA) for protein measurement following detergent solubilization. The samples were diluted in 2× Laemmli stop buffer, and the indicated amounts of protein were resolved by 10% SDS-PAGE. Blots were probed with the antibodies raised against: Tau, which includes the phosphorylation-independent antibody Tau 5 (1:1000; Chemicon International, Inc., MAB 361) and PHF-1 (1:500; a gift from Dr. P. Davies, Albert Einstein College of Medicine, Bronx, NY, USA), which recognizes the phosphorylated forms of Tau at Ser 396/404); α-Syn (1:1000; mouse monoclonal antibody; BD Transduction Laboratories, 610786); GSK-3β (1:1000; Chemicon International, Inc., AB8687); and GSK-3 (pY216; 1:1000; BD Transduction Laboratories, 612312). To confirm equal protein loading, blots were re-probed with anti-β-actin antibody (1:500; Santa Cruz Biotechnology, sc-1616).

Cell viability: The cell viability assay was performed by the MTT test (MTT = 3-(4,5-dimethylthiazol-2-yl)-2,5-diphenyltetrazolium bromide). Briefly, after cell treatment in 12 wells, cells were carefully washed twice with D-PBS and incubated for 2 h (37 °C in an atmosphere containing 5% CO_2) in the appropriate medium without serum containing 0.5 mg mL^{-1} MTT (Sigma). After two careful washes with D-PBS, formazan salts were solubilized with pure ethanol (1 mL per 12 wells), and the absorbance at $\lambda = 564$ nm was measured by UV/Vis spetrophotometry against an ethanol blank.

Statistical analysis: Cell viability results are expressed as $OD_{564} \pm$ SD as a percent of the value determined for control (vehicle-treated) cells. Statistical significance was obtained by Student *t* test.

Acknowledgements

This work was supported in part by NIH grants (NIH2-495643-440000-191100E7597 to A.P.K., and NS-34914 and NS-45326 to A.S.). We are indebted to Professor Gertrude Neumark for her generous gift to Dr. Kozikowski's research program to discover novel therapies for treating neurodegenerative diseases. We also thank Professor Peter Klein of the University of Pennsylvania and Dr. Werner Tueckmantel of Acenta Discovery, Inc. for helpful discussions.

Keywords: CNS · drug design · glycogen synthase kinase-3β · inhibitors · phosphorylation

[1] L. Meijer, M. Flajolet, P. Greengard, *Trends Pharmacol. Sci.* **2004**, *25*, 471.
[2] C. J. Phiel, C. A. Wilson, V. M. Lee, P. S. Klein, *Nature* **2003**, *423*, 435.
[3] P. S. Klein, D. A. Melton, *Proc. Natl. Acad. Sci. USA* **1996**, *93*, 8455.
[4] A. C. Hall, A. Brennan, R. G. Goold, K. Cleverley, F. R. Lucas, P. R. Gordon-Weeks, P. C. Salinas, *Mol. Cell. Neurosci.* **2002**, *20*, 257.
[5] G. H. Kuo, C. Prouty, A. DeAngelis, L. Shen, D. J. O'Neill, C. Shah, P. J. Connolly, W. V. Murray, B. R. Conway, P. Cheung, L. Westover, J. Z. Xu, R. A. Look, K. T. Demarest, S. Emanuel, S. A. Middleton, L. Jolliffe, M. P. Beavers, X. Chen, *J. Med. Chem.* **2003**, *46*, 4021.
[6] D. G. Smith, M. Buffet, A. E. Fenwick, D. Haigh, R. J. Ife, M. Saunders, B. P. Slingsby, R. Stacey, R. W. Ward, *Bioorg. Med. Chem. Lett.* **2001**, *11*, 635.
[7] H. C. Zhang, H. Ye, B. R. Conway, C. K. Derian, M. F. Addo, G. H. Kuo, L. R. Hecker, D. R. Croll, J. Li, L. Westover, J. Z. Xu, R. Look, K. T. Demarest, P. Andrade-Gordon, B. P. Damiano, B. E. Maryanoff, *Bioorg. Med. Chem. Lett.* **2004**, *14*, 3245.
[8] H. C. Zhang, C. K. Derian, D. F. McComsey, K. B. White, H. Ye, L. R. Hecker, J. Li, M. F. Addo, D. Croll, A. J. Eckardt, C. E. Smith, Q. Li, W. M. Cheung, B. R. Conway, S. Emanuel, K. T. Demarest, P. Andrade-Gordon, B. P. Damiano, B. E. Maryanoff, *J. Med. Chem.* **2005**, *48*, 1725.
[9] M. P. Coghlan, A. A. Culbert, D. A. Cross, S. L. Corcoran, J. W. Yates, N. J. Pearce, O. L. Rausch, G. J. Murphy, P. S. Carter, L. Roxbee Cox, D. Mills,

M. J. Brown, D. Haigh, R. W. Ward, D. G. Smith, K. J. Murray, A. D. Reith, J. C. Holder, *Chem. Biol.* **2000**, *7*, 793.
[10] D. Komander, G. S. Kular, A. W. Scheuttelkopf, M. Deak, K. R. Prakash, J. Bain, M. Elliott, M. Garrido-Franco, A. P. Kozikowski, D. R. Alessi, D. M. van Aalten, *Structure* **2004**, *12*, 215.
[11] W. T. O'Brien, A. D. Harper, F. Jovae, J. R. Woodgett, S. Maretto, S. Piccolo, P. S. Klein, *J. Neurosci.* **2004**, *24*, 6791.
[12] M. M. Faul, L. L. Winneroski, C. A. Krumrich, *Tetrahedron Lett.* **1999**, *40*, 1109.
[13] B. L. Mylari, W. J. Zembrowski, T. A. Beyer, C. E. Aldinger, T. W. Siegel, *J. Med. Chem.* **1992**, *35*, 2155.
[14] N. V. Savitskaya, M. N. Shchukina, *Zh. Obshch. Khim.* **1961**, *31*, 1015.
[15] M. Goedert, B. Ghetti, M. G. Spillantini, *Ann. N. Y. Acad. Sci.* **2000**, *920*, 74.
[16] D. W. Dickson, W.-K. Liu, H. Ksiezak-Reding, S. H. Yen, *Corticobasal Degeneration Adv. Neurol.* **2000**, *82*, 9.
[17] H. Braak, E. Braak, E. M. Mandelkow, *Acta Neuropathol.* **1994**, *87*, 554.
[18] K. S. Kosik, *Science* **1992**, *256*, 780.
[19] S. Lovestone, C. H. Reynolds, D. Latimer, D. R. Davis, B. H. Anderton, J. M. Gallo, D. Hanger, S. Mulot, B. Marquardt, S. Stabel, J. R. Woodgett, C. C. J. Miller, *Curr. Biol.* **1994**, *4*, 1077.
[20] M. Hong, D. C. Chen, P. S. Klein, V. M. Lee, *J. Biol. Chem.* **1997**, *272*, 25326.
[21] J. R. Munoz-Montano, F. J. Moreno, J. Avila, J. Diaz-Nido, *FEBS Lett.* **1997**, *411*, 183.
[22] A. Takashima, K. Noguchi, K. Sato, T. Hoshino, K. Imahori, *Proc. Natl. Acad. Sci. USA* **1993**, *90*, 7789.
[23] G. Alvarez, J. R. Munoz-Montano, J. Satrustegui, J. Avila, E. Bogonez, J. Diaz-Nido, *FEBS Lett.* **1999**, *453*, 260.
[24] A. Takashima, M. Murayama, O. Murayama, T. Kohno, T. Honda, K. Yasutake, N. Nihonmatsu, M. Mercken, H. Yamaguchi, S. Sugihara, B. Wolozin, *Proc. Natl. Acad. Sci. USA* **1998**, *95*.
[25] G. Yu, F. Chen, G. Levesque, M. Nishimura, D. M. Zhang, L. Levesque, E. Rogaeva, D. Xu, Y. Liang, M. Duthie, P. H. St. George-Hyslop, P. E. Fraser, *J. Biol. Chem.* **1998**, *273*, 16470.
[26] M. Murayama, S. Tanaka, J. Palacino, O. Murayama, T. Honda, X. Sun, K. Yasutake, N. Nihonmatsu, B. Wolozin, A. Takashima, *FEBS Lett.* **1998**, *433*, 73.
[27] Z. Zhang, H. Hartmann, V. M. Do, D. Abramowski, C. Sturchler-Pierrat, M. Staufenbiel, B. Sommer, M. van de Wetering, H. Clevers, P. Saftig, B. De Strooper, X. He, B. A. Yankner, *Nature* **1998**, *395*, 698.
[28] M. Hoshi, A. Takashima, K. Noguchi, M. Murayama, M. Sato, S. Kondo, Y. Saitoh, K. Ishiguro, T. Hoshino, K. Imahori, *Proc. Natl. Acad. Sci. USA* **1996**, *93*, 2719.
[29] J. J. Lucas, F. Hernandez, P. Gomez-Ramos, M. A. Moran, R. Hen, J. Avila, *EMBO J.* **2001**, *20*, 27.
[30] L. Otvos, Jr., L. Feiner, E. Lang, G. I. Szendrei, M. Goedert, V. M. Lee, *J. Neurosci. Res.* **1994**, *39*, 669.
[31] F. Hernandez, J. Borrell, C. Guaza, J. Avila, J. J. Lucas, *J. Neurochem.* **2002**, *83*, 1529.
[32] A. Gaomez-Ramos, X. Abad, M. Laopez Fanarraga, R. Bhat, J. C. Zabala, J. Avila, *Brain Res.* **2004**, *1007*, 57.
[33] M. Pap, G. M. Cooper, *J. Biol. Chem.* **1998**, *273*, 19929.
[34] D. A. Cross, A. A. Culbert, K. A. Chalmers, L. Facci, S. D. Skaper, A. D. Reith, *J. Neurochem.* **2001**, *77*, 94.
[35] G. N. Bijur, P. De Sarno, R. S. Jope, *J. Biol. Chem.* **2000**, *275*, 7583.
[36] W. Dauer, N. Kholodilov, M. Vila, A. C. Trillat, R. Goodchild, K. E. Larsen, R. Staal, K. Tieu, Y. Schmitz, C. A. Yuan, M. Rocha, V. Jackson-Lewis, S. Hersch, D. Sulzer, S. Przedborski, R. Burke, and R. Hen, *Proc. Natl. Acad. Sci. USA* **2002**, *99*, 14524.
[37] O. M. Schleuter, F. Fornai, M. G. Alessandri, S. Takamori, M. Geppert, R. Jahn, T. C. Seudhof, *Neuroscience* **2003**, *118*, 985.
[38] F. J. Lee, F. Liu, Z. B. Pristupa, H. B. Niznik, *FASEB J.* **2001**, *15*, 916.
[39] J. Lotharius, P. Brundin, *Hum. Mol. Genet.* **2002**, *11*, 2395.
[40] R. G. Perez, J. C. Waymire, E. Lin, J. J. Liu, F. Guo, M. J. Zigmond, *J. Neurosci.* **2002**, *22*, 3090.
[41] R. E. Drolet, B. Behrouz, K. J. Lookingland, J. L. Goudreau, *Neurotoxicology* **2004**, *25*, 761.
[42] K. Hughes, E. Nikolakaki, S. E. Plyte, N. F. Totty, J. R. Woodgett, *EMBO J.* **1993**, *12*, 803.
[43] D. Blum, S. Torch, N. Lambeng, M. Nissoi, A. L. Benabid, R. Sadoul, J. M. Verna, *Prog. Neurobiol.* **2001**, *65*, 135.
[44] R. V. Bhat, J. Shanley, M. P. Correll, W. E. Fieles, R. A. Keith, C. W. Scott, C. M. Lee, *Proc. Natl. Acad. Sci. USA* **2000**, *97*, 11074.
[45] M. Hetman, J. E. Cavanaugh, D. Kimelman, Z. Xia, *J. Neurosci.* **2000**, *20*, 2567.
[46] G. I. Welsh, J. C. Patel, C. G. Proud, *Anal. Biochem.* **1997**, *244*, 16.
[47] SYBYL 7.0, Tripos, Inc., 1699 South Hanley Rd., St. Louis, MO 63144, USA, **2004**.
[48] B. R. Brooks, R. E. Bruccoleri, B. D. Olafson, D. J. States, S. Swaminathan, M. Karplus, *J. Comput. Chem.* **1983**, *4*, 187.
[49] K. C. Nicolaou, R. M. Rodriguez, H. J. Mitchell, F. L. van Delft, *Angew. Chem. Int. Ed.* **1998**, *37*, 1874.
[50] Accelrys Inc., 9685 Scranton Rd., San Diego, CA 92121-3752, USA, **2003**.
[51] P. H. Olesen, A. R. Sorensen, B. Urso, P. Kurtzhals, A. N. Bowler, U. Ehrbar, B. F. Hansen, *J. Med. Chem.* **2003**, *46*, 3333.
[52] I. Hers, J. M. Tavarae, R. M. Denton, *FEBS Lett.* **1999**, *460*, 433.
[53] M. Leost, C. Schultz, A. Link, Y. Z. Wu, J. Biernat, E. M. Mandelkow, J. A. Bibb, G. L. Snyder, P. Greengard, D. W. Zaharevitz, R. Gussio, A. M. Senderowicz, E. A. Sausville, C. Kunick, L. Meijer, *Eur. J. Biochem.* **2000**, *267*, 5983.
[54] S. Leclerc, M. Garnier, R. Hoessel, D. Marko, J. A. Bibb, G. L. Snyder, P. Greengard, J. Biernat, Y. Z. Wu, E. M. Mandelkow, G. Eisenbrand, L. Meijer, *J. Biol. Chem.* **2001**, *276*, 251.
[55] L. Meijer, A. M. Thunnissen, A. W. White, M. Garnier, M. Nikolic, L. H. Tsai, J. Walter, K. E. Cleverley, P. C. Salinas, Y. Z. Wu, J. Biernat, E. M. Mandelkow, S. H. Kim, G. R. Pettit, *Chem. Biol.* **2000**, *7*, 51.
[56] J. A. Bertrand, S. Thieffine, A. Vulpetti, C. Cristiani, B. Valsasina, S. Knapp, H. M. Kalisz, M. Flocco, *J. Mol. Biol.* **2003**, *333*, 393.
[57] R. Bhat, Y. Xue, S. Berg, S. Hellberg, M. Ormeo, Y. Nilsson, A. C. Radeseater, E. Jerning, P. O. Markgren, T. Borgegeard, M. Nyleof, A. Gimaenez-Cassina, F. Hernandez, J. J. Lucas, J. Diaz-Nido, J. Avila, *J. Biol. Chem.* **2003**, *278*, 45937.
[58] Y. Maeda, M. Nakano, H. Sato, Y. Miyazaki, S. L. Schweiker, J. L. Smith, A. T. Truesdale, *Bioorg. Med. Chem. Lett.* **2004**, *14*, 3907.
[59] C. Bissantz, G. Folkers, D. Rognan, *J. Med. Chem.* **2000**, *43*, 4759.
[60] R. D. Clark, A. Strizhev, J. M. Leonard, J. F. Blake, J. B. Matthew, *J. Mol. Graphics Modell.* **2002**, *20*, 281.
[61] R. Wang, S. Wang, *J. Chem. Inf. Comput. Sci.* **2001**, *41*, 1422.
[62] P. A. Petukhov, A. N. Pae, *Abstracts of Papers*, *230th ACS National Meeting*, Washington, DC, **2005**, pp. COMP.

Received: September 7, 2005

